PEAK POINT DESCRIPTION UTILIZING OF AN ARTIFICIAL NEURAL NETWORK APPROACH IN COMPARISON WITH THE COMMONLY USED RELATIONSHIPS

Petr OPĚLA [1], Ivo SCHINDLER [1], Stanislav RUSZ [1], Vojtěch ŠEVČÁK [1]

[1]VSB - Technical University of Ostrava, Ostrava, Czech Republic, EU
petr.opela@vsb.cz

Abstract

The peak point coordinates (i.e. peak stress, peak strain) play a significant role in case of a flow curve description. These coordinates are strongly dependent on the temperature and strain rate, so they need to be related to these thermomechanical circumstances before use in the flow stress models. In this research, the experimental peak point coordinates of the C45 and 38MnVS6 steels were described in a wide range of thermomechanical conditions by use of two different methodologies. The first one was based on the ordinary predictive relationships utilizing the well-known Zener-Hollomon parameter. The second one was based on the artificial neural network approach. The aim was to compare appropriateness of these methods. The results have suggested better aptness in case of the assembled neural networks.

Keywords: Peak point coordinates, predictive relationship, artificial neural network

INTRODUCTION

The peak point coordinates (i.e. peak stress, σ_p, and peak strain, ε_p) describe the maximum flow stress level (peak point) of hot flow curves; see **Figure 1** [1]. It is well known, these curves express the dependence of natural flow stress of formed (e.g. rolled, forged, etc.) material on the magnitude of strain under various levels of thermomechanical conditions (i.e. strain rates, temperatures). Flow curves are commonly assembled from the experimentally acquired data (based on compression or torsion tests) [2].

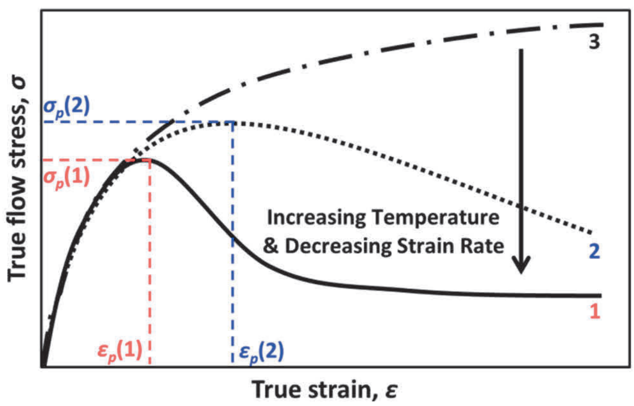

Figure 1 Examples of hot flow curve types and related peak point coordinates [1]

Experimentally compiled curves are usually mathematically described because of further computer simulations. The peak point coordinates then play a substantial role in case of this description - they are implemented into the so-called flow stress models [3]. The peak point coordinates are dependent on the magnitude of strain rate and temperature - that means they need to be related to these thermomechanical variables before use in the flow stress models. Different approaches can be then used to describe these coordinates. Commonly used methodology utilizes the known predictive relationships, which can be treated by regression methods [4]. These relationships usually relate the examined coordinates to the well-known Zener-Hollomon parameter (connecting the mutual effect of temperature and strain rate). Another (often more reliable) approach is to use of intelligent algorithms, such as artificial neural networks (ANN) [5]. The aim of this paper is to compare reliability of commonly used equations of peak point description with the artificial neural network approach. Experimental values of the peak point coordinates of the C45 and 38MnVS6 steels will be used for the purpose of this investigation.

1. EXPERIMENTAL MATERIALS

The experimental peak point coordinates of the C45 medium-carbon steel and of 38MnVS6 micro-alloyed steel were obtained from the experimental flow curves of the examined steels. These curves were assembled on the basis of the uniaxial hot compression datasets. Whole experimental procedure was in detail described previously in [6] for the C45 steel and [7] in case of the 38MnVS6 steel, respectively. The range of the tested thermomechanical conditions of the C45 steel was as follows: Temperatures of 1553 K, 1473 K, 1373 K, 1273 K and 1173 K and the strain rates of 0.1 s^{-1}, 1 s^{-1}, 10 s^{-1} and 100 s^{-1}. The range of the tested thermomechanical conditions of the 38MnVS6 steel was as follows: Temperatures of 1553 K, 1473 K, 1373 K, 1273 K and 1123 K and the strain rates of 0.1 s^{-1}, 1 s^{-1}, 10 s^{-1} and 100 s^{-1}. So, there are twenty combinations of the thermomechanical parameters (thus twenty peak point coordinates) for the both examined steels.

2. PEAK POINT DESCRIPTION BY THE COMMONLY USED RELATIONSHIPS

The peak point coordinates, i.e. the peak strain, ε_p (-), and the corresponding peak stress, σ_p (MPa), see **Figure 1**, belong to the temperature, T (K), and strain rate, $\dot{\varepsilon}$ (s^{-1}), dependent parameters. Mutual effect of these variables is commonly expressed by the Zener-Hollomon parameter, Z (s^{-1}) [8]:

$$Z = \dot{\varepsilon} \cdot \exp\left(\frac{Q}{R \cdot T}\right) \quad (1)$$

The R (8.314 $J \cdot K^{-1} \cdot mol^{-1}$) is the universal gas constant, and Q ($J \cdot mol^{-1}$) is the hot deformation activation energy. The peak strain and peak stress values could be then described in wide range of thermomechanical conditions as follows from the equations (2) and (3) [9]:

$$\varepsilon_p = a \cdot Z^b \quad (2)$$

$$\sigma_p = \frac{1}{\alpha} \cdot \operatorname{arcsinh} \sqrt[n]{\frac{Z}{A}} \quad (3)$$

In the above mentioned equations, A (s^{-1}), a (-), b (-), n (-) and α (MPa^{-1}) are material constants. The calculation of a and b is treated by regression analysis of the equation (2). The calculation of A, n, Q and α can be done by the regression analysis of Garofalo equation; in detail discussed in [9].

The values of ε_p and σ_p were calculated for all sets of the thermomechanical circumstances of the both examined steels via the equations (2) and (3). All required material constants of these equations are presented in **Table 1**.

Table 1 Material constants of the relationships predicting the peak point coordinates

Material	A (s^{-1})	a (-)	b (-)	n (-)	Q ($kJ \cdot mol^{-1}$)	α (MPa^{-1})
C45	$3.96 \cdot 10^{11}$	$3.3 \cdot 10^{-3}$	0.2	4.3	292	$9.5 \cdot 10^{-3}$
38MnVS6	$3.25 \cdot 10^{12}$	$2.5 \cdot 10^{-3}$	0.2	4.6	316	$8.6 \cdot 10^{-3}$

3. PEAK POINT DESCRIPTION BY AN ARTIFICIAL NEURAL NETWORK APPROACH

An artificial neural network (ANN) approach belongs among so-called intelligent algorithms. These methods bring remarkable results on the field of nonlinear tasks [5, 10]. Multi-layer Feed-Forward Artificial Neural Network with the Back-Propagation (BP) learning algorithm is the most used type of ANN in case of the material modeling [11, 12]. This type of ANN was used to create four neural networks - two networks for each of the examined steels (always one network to predict of e_p-values and one to predict of σ_p-values). Architecture of the created networks was quite simple. Each network connects the input variables (temperature and strain rate) with the output variable (peak strain or peak stress) via set of artificial neurons arranged in three layers, see **Figure 2**. The input layer includes two neurons. These neurons are associated with the vectors of the input variables - no calculations run inside of them. The neurons of the input layer are connected with the neurons in the one hidden layer via set of synaptic weights (w_{ij}), and the neurons of the hidden layer are then connected with the one neuron in the output layer via another set of weights (w_{jk}) (the output of this neuron is the vector of predicted output variable). Each neuron of the hidden and output layer is further linked with a unique bias value (b_j, b_k). Neurons of the hidden and output layer are activated by the proper transfer function; nonlinear in case of the hidden layer and pure linear in the output layer, respectively. The processes inside of the network can be divided in two basic steps. The first one is the feed-forward of the function signal; mathematically described in [13]. The second one is the back-propagation of an error signal to enable the following network training [14].

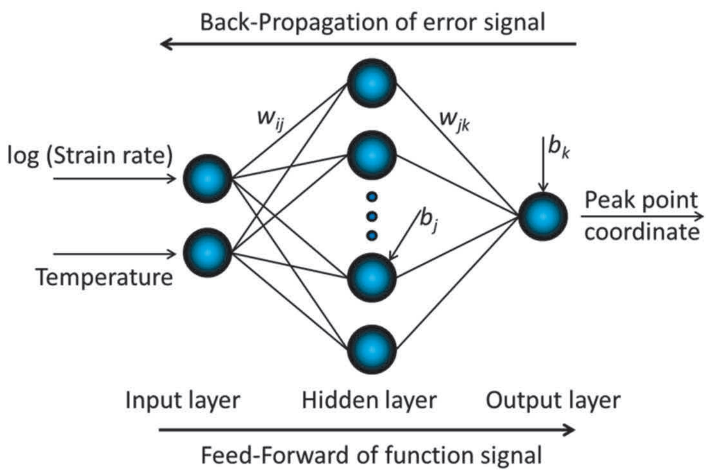

Figure 2 Schematic illustration of the used artificial neural network architecture

The aim of the network training is to minimize a performance function to achieve reliable results. In this research, the performance function was set as the mean square error (MSE) [12]:

$$\mathrm{MSE} = \frac{1}{n} \cdot \sum_{i=1}^{n} (E_i)^2 \quad (4)$$

The n represents the number of data points involved in calculations, E_i is the i-th absolute error of the output layer neuron (i.e. difference between the network output and target value) [12]. The minimization process involves a searching of an appropriate set of the weights and biases to get a low MSE value [14]. The process of minimization was performed by the Levenberg-Marquardt optimization algorithm [15, 16].

However, as the very first step (before the network assembly), it is highly important to split the experimental dataset into three parts - Training set (ca. 60 %) to train the network, Validation set (ca. 20 %) to validate network response during training process, and Testing set (ca. 20 %) to verify the network prediction capability out of the training range [17]. **Table 2** clearly shows the split of datasets of the experimental values of the examined steels - **training set**, **validation set** and **testing set**, respectively.

Table 2 Split of the datasets of the experimental values of peak point coordinates

C45 / 38MnVS6	1553 K	1473 K	1373 K	1273 K	1173 K / 1123 K
0.1 s^{-1}	X	X	X	X	X
1 s^{-1}	X	X	X	X	X
10 s^{-1}	X	X	X	X	X
100 s^{-1}	X	X	X	X	X

It must be mentioned that the values of the input variables entering the input layer are distributed in distinct ranges and even dimensions. This fact then leads to a poor convergence speed and prediction accuracy of neural network. Therefore, it is important to normalize these data to ensure they will be dimensionless and in an approximately same magnitude [13]. In this research, the normalization process was performed as described in [17, 18].

The key factor influencing the network performance is the number of neurons in the hidden layer. To determine an ideal number of hidden neurons it is necessary to train the network for various numbers of neurons in the hidden layer. Then, it is possible, based on the returned results, to reveal an appropriate form of the network architecture [12, 13]. **Figure 3** graphically displays the influence of neuron number in the hidden layer on the magnitude of MSE for the case of the each trained network. The appropriate number of hidden neurons of given network is, of course, clearly identified by the lowest value of MSE.

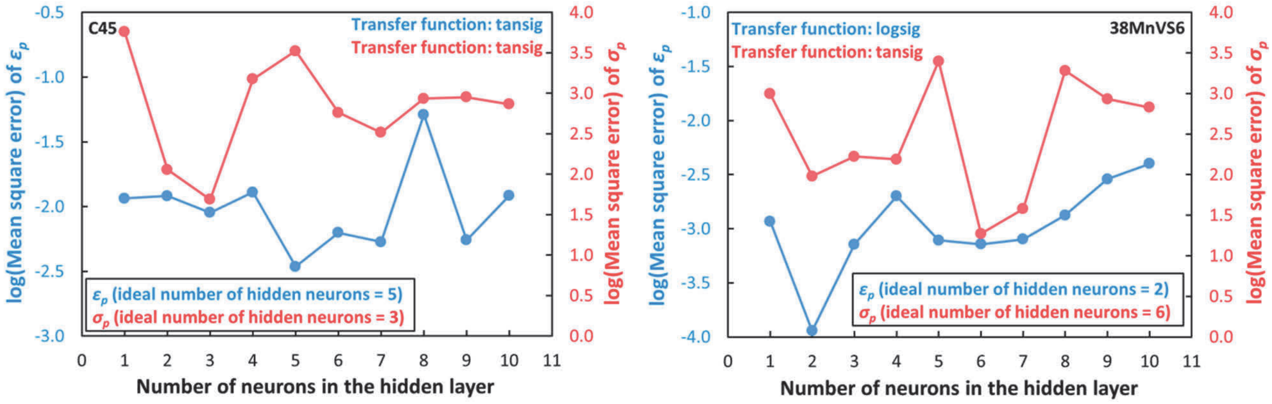

Figure 3 Performance of the assembled artificial neural networks at different hidden neuron levels

4. ASSESSMENT OF THE PERFORMANCE OF SURVEYED APPROACHES

In order to evaluate the prediction capability of the examined approaches, the relative percentage error, η (%), is introduced to compare deviations between experimental and calculated peak point coordinates in case of each combination of temperature and strain rate. The *i*-th error, η_i (where $i = [1, 20] \subset \mathbb{N}$), is expressed as [12]:

$$\eta_i = \frac{y(x_i) - y_i}{y_i} \cdot 100 \qquad (5)$$

In the equation (5), y_i is the *i*-th experimental value of an examined peak point coordinate and the $y(x_i)$ is the *i*-th calculated value [12]. The η-values of the peak point coordinates are compared in case of both approaches in **Figure 4**. In case of the 38MnVS6 steel, the η-values of the peak strain are held below of 10% border with regard to the ANN approach. While, in case of equation (2), the 10% border is overcome in many cases - in one case, the η-value reaches even of 67.80 %. Similar behavior can be observed also in case of the C45 steel. In case of the ANN approach, the η-values of the peak strain, with exception of three cases, are again held below of 10% border. With regard to equation (2), almost all of the η-values are out of the 10% range, and one of them reaches even of 60.44 %. Quite different behavior can be observed with regard to the description of the peak stress values. It seems like using the classic equation (3) brings slightly better performance then ANN approach. Note, the larger range of η-values does not mean the poorer performance. For this reason, two other indicators, namely average value of η-values (μ) and standard deviation (σ), are further used to augment the evaluation [12]:

$$\mu = \frac{1}{n} \cdot \sum_{i=1}^{n} \eta_i \qquad (6)$$

$$\sigma = \sqrt{\frac{1}{n} \cdot \sum_{i=1}^{n} (\eta_i - \mu)^2} \tag{7}$$

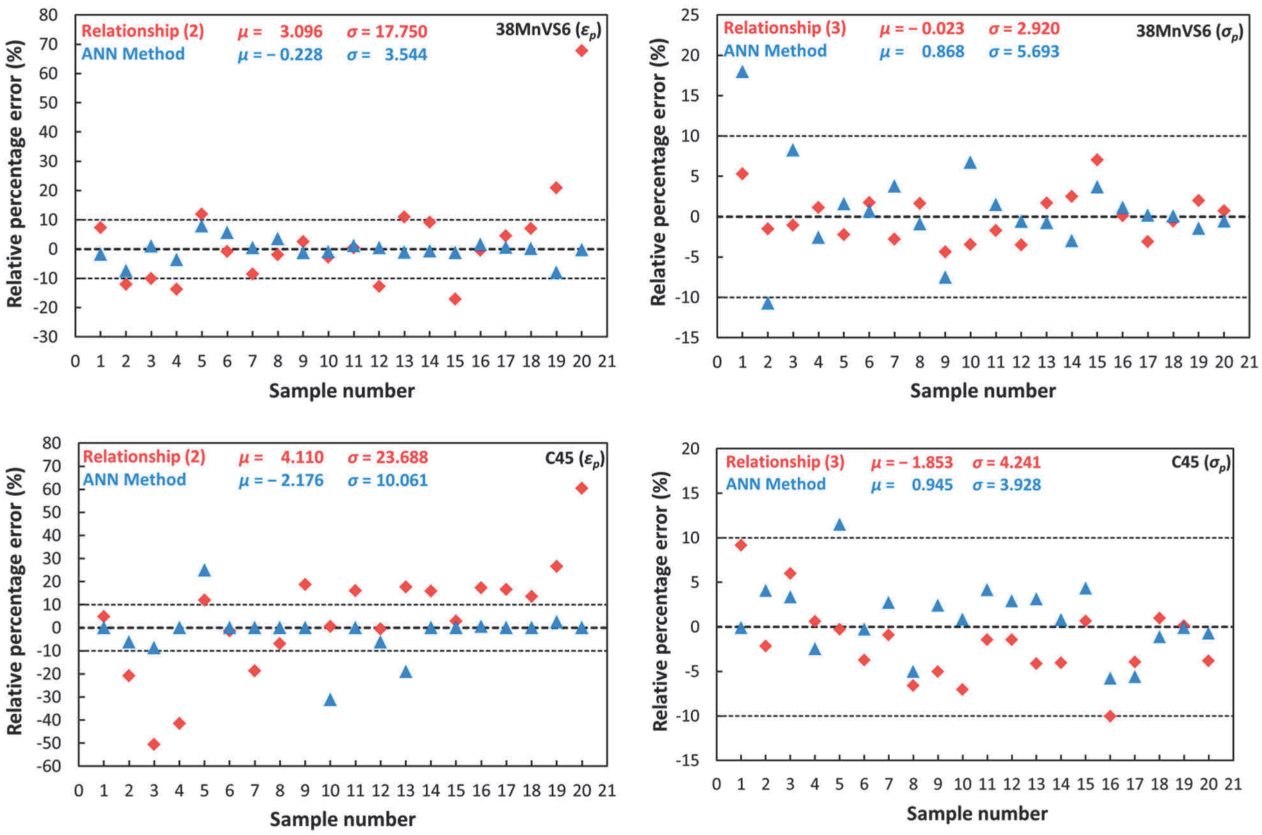

Figure 4 Comparison of relative percentage error of predicted values of the peak point coordinates with the experimentally acquired

The *n* is the sample number of relative percentage error (n = 20). Average value, μ, measures the magnitude of the dataset, whereas standard deviation, σ, denotes the degree of dispersion and provides an idea of how close the entire dataset is to the average value. The μ-value going to zero and low value of σ imply high accuracy of description [12]. As shown in **Figure 4**, μ-values and σ-values of the ANN description are more favorable in comparison with the standard equations (2) and (3). However, the exception can be found in case of the peak stress description with respect to 38MnVS6 steel. This fact is confirmed by the graphical presentation of the η-scatter.

5. CONCLUSION

Peak point coordinates (i.e. peak strain and peak stress) of the experimental flow curves of the C45 and 38MnVS6 steels were mathematically described by two different approaches. The first one is based on the widely used relationships describing the peak point coordinates with respect to the well-known Zener-Hollomon parameter (connecting the mutual effect of temperature and strain rate). The second one utilizes the multi-layer feed-forward artificial neural networks with the back-propagation learning algorithm. It can be concluded, based on the achieved results, the neural network approach exhibits mostly better prediction capability. So, the peak point coordinates predicted by the neural network approach can be then appropriate to use in the process of modeling of given flow curves via known flow stress models.

ACKNOWLEDGEMENTS

This paper was created on the Faculty of Metallurgy and Materials Engineering in the Project No. LO1203 "Regional Materials Science and Technology Centre - Feasibility Program" funded by Ministry of Education, Youth and Sports of the Czech Republic.

REFERENCES

[1] EBRAHIMI, R. and SOLHJOO, S. Characteristic Points of Stress-Strain Curve at High Temperature. *International Journal of ISSI*. 2007. vol. 4, no. 1-2, pp. 24-27.

[2] EBRAHIMI, R. and SHAFIEI, E. Mathematical Modeling of Single Peak Dynamic Recrystallization Flow Stress Curves in Metallic Alloys. In: SZTWIERTNIA, K., ed. *Recrystallization* [online]. Rijeka: InTech, 2012. Chapter 9, pp 207-225 [viewed 2018-03-14]. Available from: http://www.intechopen.com/books/recrystallization/mathematical-modeling-of-single-peak-dynamic-recrystallization-flow-stress-curves-in-metallic-alloys.

[3] GRONOSTAJSKI, Z. The constitutive equations for FEM analysis. *Journal of Materials Processing Technology*. 2000. vol. 106, no. 1-3, pp. 40-44.

[4] SHAFAAT, M. A., OMIDVAR, H. and FALLAH, B. Prediction of hot compression flow curves of Ti-6Al-4V alloy in α + β phase region. *Materials & Design*. 2011. vol. 32, no. 10, pp. 4689-4695.

[5] WU, S. W., ZHOU, X. G., CAO, G. M., LIU, Z. Y. and WANG, G. D. The Improvement on Constitutive Modeling of Nb-Ti Micro Alloyed Steel by Using Intelligent Algorithms. *Materials & Design*. 2017. vol. 116, pp. 676-685.

[6] OPĚLA, P., SCHINDLER, I., KAWULOK, P., VANČURA, F., KAWULOK, R., RUSZ, S. and PETREK, T. Hot Flow Stress Models of the Steel C45. *Metalurgija*. 2015. vol. 54, no. 3, pp. 469-472.

[7] OPĚLA, P., SCHINDLER, I., KAWULOK, P., VANČURA, F., KAWULOK, R. and RUSZ, S. New Model Predicting Flow Curves in Wide Range of Thermomechanical Conditions of 38MnVS6 Steel. In *METAL 2016: 25th Anniversary International Conference on Metallurgy and Materials*. Brno: TANGER, 2016, pp. 458-463.

[8] ZENER, C. and HOLLOMON, J. H. Effect of Strain Rate upon Plastic Flow of Steel. *Journal of Applied Physics*. 1944. vol. 15, no. 1, pp. 22-32.

[9] SCHINDLER, I. and BOŘUTA, J. *Utilization Potentialities of the Torsion Plastometer*. Żory: OLDPRINT, 1998. p. 140.

[10] YAN, J., PAN, Q. L., LI, A. D. and SONG, W. B. Flow Behavior of Al-6.2Zn-0.70Mg-0.30Mn-0.17Zr Alloy during Hot Compressive Deformation Based on Arrhenius and ANN models. *Transaction of Nonferrous Metals Society of China*. 2017. vol. 27, pp. 638-647.

[11] MA, X., ZENG, W., TIAN, F., Sun, Y. and ZHOU, Y. Modeling Constitutive Relationship of BT25 Titanium Alloy during Hot Deformation by Artificial Neural Network. *Journal of Materials Engineering and Performance*. 2012. vol. 21, no. 8, pp. 1591-1597.

[12] QUAN, G. Z., ZOU, Z. Y., WANG, T., LIU, B. and LI, J. Ch. Modeling the Hot Deformation Behaviors of As-Extruded 7075 Aluminum Alloy by an Artificial Neural Network with Back-Propagation Algorithm. *High Temperature Materials and Processes*. 2017. vol. 36, no. 1, pp. 1-13.

[13] LV, J., REN, H. and GAO, K. Artificial Neural Network-based Constitutive Relationship of Inconel 718 Superalloy Construction and Its Application in Accuracy Improvement of Numerical Simulation. *Applied Sciences*. 2017. vol. 7, no. 2, pp. 124-141.

[14] Principles of Training Multi-Layer Neural Network Using Back propagation [online]. Update: sept. 2004. [viewed 2018-03-14]. Available from: http://home.agh.edu.pl/~vlsi/AI/backp_t_en/backprop.html.

[15] LEVENBERG, K. A Method for the Solution of Certain Non-Linear Problems in Least Squares. *Quarterly of Applied Mathematics*.1944. vol. 2, no. 2, pp. 164-168.

[16] MARQUARDT, D. W. An Algorithm for Least-Squares Estimation of Nonlinear Parameters. *Journal of the Society for Industrial and Applied Mathematics*. 1963. vol. 11, no. 2, pp. 431-441.

[17] SCHMID, M. D. A Neural Network Package for Octave - User's Guide [online]. Version: 0.1.9.1. [viewed 2018-03-14]. Available from: https://mafiadoc.com/a-neural-network-package-for-octave-user39s-guide-version-0191_59b4e5641723dddcc6daf493.html.

[18] Prestd [online]. Neural Network Toolbox™ [viewed 2018-03-14]. Available from: http://cens.ioc.ee/local/man/matlab/toolbox/nnet/prestd.html.